A Bayesian Method for Very High Resolution Multi Aspect Angle Radargrammetry

Kanika Goel (1,2), Nico Adam (1)

(1) German Aerospace Center (DLR), Remote Sensing Technology Institute (IMF), Germany
(2) Technische Universität München (TUM), Lehrstuhl für Methodik der Fernerkundung, Germany

Abstract

InSAR's capabilities have been considerably improved by advanced processing techniques such as Persistent Scatterer Interferometry (PSI) and SAR Tomography (TomoSAR). However, complicated scattering situations (e.g. layover) need to be better resolved in urban areas. This paper presents a new technique for providing the 3D point scatterer location and the resolution cell configuration, based only on the amplitude of SAR images. The implemented method is based on the principle of radargrammetry and uses Bayesian inference. As compared to PSI and TomoSAR, the method is insensitive to temporal decorrelation, atmospheric phase screen (APS) and non-linear motion of point scatterers.

1 Introduction

InSAR is well established for mapping of urban areas and buildings. In the last few years, InSAR's capabilities have been considerably improved. By using large stacks of SAR images acquired over the same area instead of the classical two images used in the standard configurations, long time series can be analyzed and the baseline spread allows to form a synthetic aperture in elevation. These coherent techniques that have been developed are Persistent Scatterer Interferometry (PSI) and SAR Tomography (TomoSAR). With PSI, it is now possible to monitor deformations of urban areas and buildings with a precision better than one millimeter per year [1]. The technique exploits long time coherent (phase stable) scatterers and restricts the estimation to these points given by chance [1], [2]. In TomoSAR, a real three-dimensional imaging of a scene is achieved by the formation of an additional synthetic aperture in elevation by a coherent combination of images acquired from several parallel tracks [3], [4], [5]. Here, the 3-D radar reflectivity function is estimated. However, both these techniques are coherent and thus, have some limitations caused by temporal decorrelation, the atmospheric phase screen (APS) and non-linear displacement.

Consequently, both PSI and TomoSAR need to be better supported. For example, the scatterer configuration can be made available beforehand. It allows resolving complicated scattering situations such as layover in urban areas, which is a problem especially for high resolution SAR. The scatterer configuration detection and finally, unambiguous height estimation requires precise DEM information which is usually not available on this scale. An approach to solve this problem has been presented in this paper. The aim is to estimate the 3D scatterer location and resolution cell configuration using a method which is only amplitude based and is insensitive to temporal decorrelation, APS and non-linear displacement. The implemented method is based on the principle of radargrammetry [6], [7] i.e. change of slant range distance due to varying incidence angles. The proposed method makes use of Bayesian inference using directed graphs. Probability density functions (pdfs) are modelled using particle representations. The estimation method is demonstrated on high resolution spotlight data of the German radar satellite TerraSAR-X.

2 Radargrammetry

2.1 Principle of Radargrammetry

The radargrammetry principle is based on the change of slant range distance caused by varying incidence angles. It makes use of SAR amplitude images only. Point scatterers with a certain height are mapped into different range locations of the SAR scene. This is illustrated in Figure 1, where we have three TerraSAR-X images of Swissotel Berlin, taken from incidence angles of 27.1, 37.8 and 45.8 degrees respectively from left to right. We can see clearly that there is a shift of the scatterers in slant range direction because of the varying incidence angles. This shift is more with increasing heights of the scatterers (with no shift for scatterers on the ground).

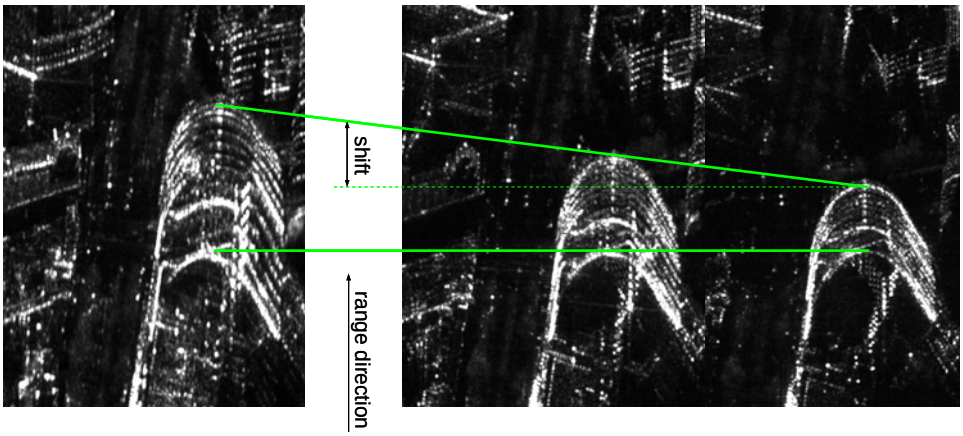

Figure 1: Shift in slant range direction for point scatterers on the building due to varying incidence angles.

2.2 Height Estimation Principle

Mathematically, to estimate the heights of point scatterers using the radargrammetry principle, we have to consider two geometrical effects in range direction.
The first effect is the SAR coregistration. When SAR images are taken from different incidence angles, the images are not aligned due to differences in imaging geometry. Thus, alignment of all SAR images has to be done with respect to a master scene. In range direction, this is achieved by shifting and scaling the images. This is called coregistration and the resolution cells on the ground with zero height get aligned in the stack of acquisitions. When a point on the ground is projected on the master scene, the master slant range distance is Δr_m. When the same point is projected on the slave scene, the slave slant range distance is Δr_s. Now coregistration shifts and scales the point on slave image so that Δr_m and Δr_s correspond to the same distance on the ground. The slave slant range distance becomes equal to $\Delta r_s^m = \Delta r_m$, and is given by:

$$\Delta r_s^m = \Delta r_m = \frac{\sin(\theta_m)}{\sin(\theta_s)} \cdot \Delta r_s \qquad (1)$$

where θ_m and θ_s are master scene and slave scene incidence angles respectively. The effect of coregistration is visualized in Figure 2.

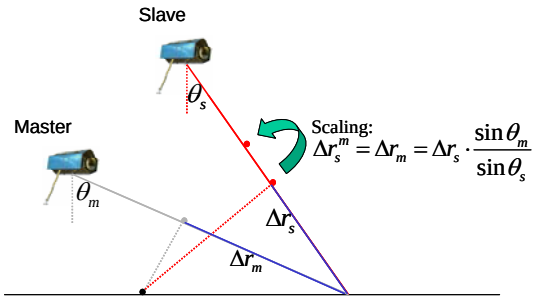

Figure 2: Geometric effect of coregistration.

We also have to consider the geometric effect caused by the height of a scatterer. When a point at a height h gets projected on the master scene, the master slant range distance is given by $\Delta r_m = h \cdot \cos(\theta_m)$. And when it gets projected on the slave scene, the slave slant range distance is $\Delta r_s = h \cdot \cos(\theta_s)$. Now due to coregistration, the slave slant range distance becomes equal to Δr_s^m, which is given by:

$$\Delta r_s^m = \frac{\sin(\theta_m)}{\sin(\theta_s)} \cdot \Delta r_s \qquad (2)$$

where $\Delta r_s = h \cdot \cos(\theta_s)$. Now Δr_s^m is not equal to Δr_m because of the height of the scatterer i.e. the zero height related coregistration also influences the scatterers with a certain height h and we can measure a relative shift of the scatterers with respect to the master scene. This effect is shown in Figure 3.

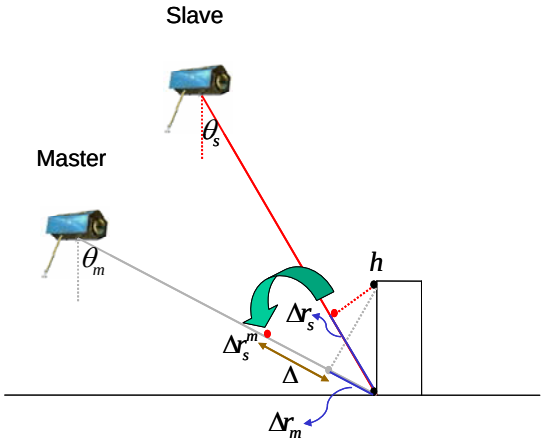

Figure 3: Geometric effect of height of a scatterer.

The relative shift Δ of the scatterer with respect to the master scene is given by:

$$\Delta = \Delta r_s^m - \Delta r_m \qquad (3)$$

where $\Delta r_m = h \cdot \cos(\theta_m)$ i.e.

$$\Delta = \frac{\sin(\theta_m - \theta_s)}{\sin\theta_s} \cdot h = f_{h2\Delta} \cdot h \qquad (4)$$

where $f_{h2\Delta}$ is the *height to relative shift factor*. The relative shift Δ (in units of meters) is linearly dependent on the height h of the point scatterer by this factor $f_{h2\Delta}$. This shift in range direction for point scatterers (at a height h) is used for the unambiguous height estimation. This is explained in section 2.3 of this paper.

2.3 Implementation using Bayesian Inference

The framework implemented for height estimation of point scatterers is based on Bayesian inference using directed graphs. The height estimation problem for a scatterer can be converted to the following line equation:

$$\Delta^{beam\_i} = f_{h2\Delta}^{beam\_i} \cdot h \qquad (5)$$

where Δ^{beam_i} is the relative shift in range direction for beam i with respect to the master beam; $f_{h2\Delta}^{beam\_i}$ is the *height to relative shift factor* for beam i; h is the height of the scatterer and i = 1,2,…,N, where N is the number of beams. Also, there might be small misregistrations in range and azimuth directions, which we represent by Δrg^{beam_i} and Δaz^{beam_i}.

The relative shift Δ^{beam_i} is dependent on the height of the scatterer h, *height to relative shift factor* $f_{h2\Delta}^{beam\_i}$, misregistration in range direction Δrg^{beam_i} and misregistration in azimuth direction Δaz^{beam_i}. Considering all the parameters as random variables (RVs), we can construct the directed graphical model for the problem as shown in Figure 4. Note that h, Δrg^{beam_i} and Δaz^{beam_i} are the RVs to be estimated, $f_{h2\Delta}^{beam\_i}$ is the known variable and Δ^{beam_i} is the observed variable (intensity along the range line is taken as the likelihood for a certain point scatterer offset).

The azimuth misregistration (Δaz^{beam_i}) includes two terms. First term is the height independent misregistration of the point scatterers, denoted by $\Delta az_1^{beam\_i}$. The second term is the height and incident angle dependent shift in azimuth direction (this term is very small compared to the shift in range direction), denoted by $\Delta az_2^{beam\_i}(h,\theta)$.

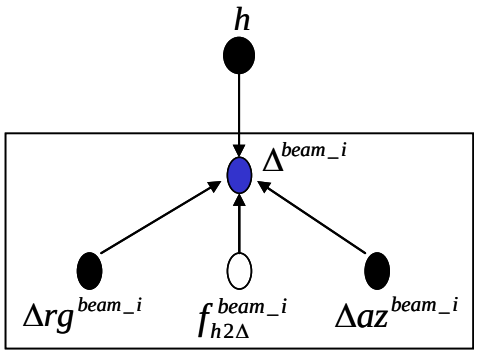

Figure 4: Directed graphical model for height estimation of point scatterers.

The implemented framework maximizes the posterior probability of the estimated height h_{MAP} given the likelihood of the offset measurements $f(\Delta^{beam1,2,3} \mid h, \Delta rg^{beam1,2,3}, \Delta az^{beam1,2,3}, f_{h2\Delta}^{beam1,2,3})$. Thus, the height estimation is a simple Bayesian line fitting problem involving multimodal pdfs. The pdfs are modelled using particle representations.

Figure 5 illustrates the line fitting. There are three beams in this figure, with several scenes per beam (to reduce speckle). We detect a point scatterer in the master scene, and then try to fit a line through the other scenes for that point scatterer, starting from this point. If the point scatterer is on the fitted line in each scene, the slope of that line corresponds to the estimated absolute height.

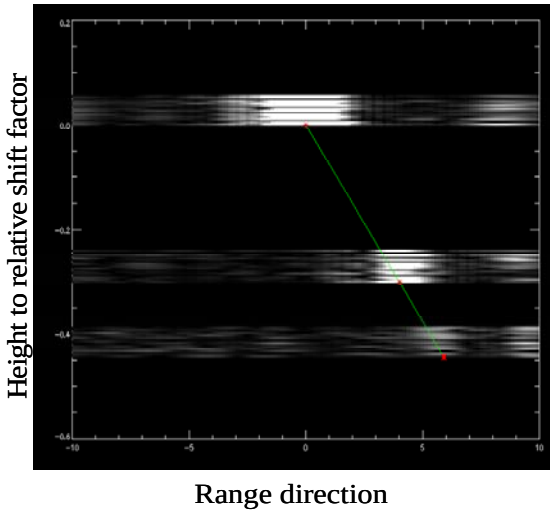

Figure 5: Height estimation of point scatterers using Bayesian inference.

2.4 Joint Estimation of Point Scatterer Cloud

The technique was improved by performing joint estimation of a small neighbourhood i.e. point scatterers located on the same range line close to each other. The joint estimation models two hypotheses. First, we assume that the scatterers are located on a vertical wall. Second, we assume that they are located on a horizontal surface (e.g. the ground). We estimate the evidence for each case, and select the model with the higher evidence. Bayesian inference is again used for joint estimation. For evidence calculation, Monte Carlo integration is used.

3 Application Test Case

The practically implemented framework has been tested using high resolution spotlight 300 MHz TerraSAR-X scenes of Berlin covering the central station. Four beams at incidence angles of 27.52, 38.11,

45.98 and 51.74 degrees are used. Several scenes per beam i.e. with a similar incidence angle are used to reduce speckle. Figure 6 shows the height estimation results as visualized in Google Earth for the Berlin central station.

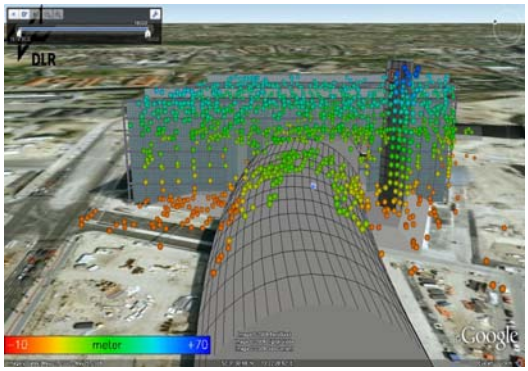

Figure 6: Height estimation results for Berlin central station.

The likelihood of height for a point on the building is shown in Figure 7. The width of the single peak provides information about the precision of height estimation.

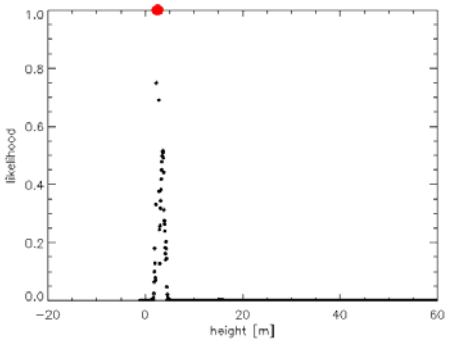

Figure 7: Likelihood of height for a point scatterer on the building.

In case of multiple scatterers in a resolution cell, multiple peaks at corresponding heights can be found. This case is illustrated in Figure 8 for a point scatterer on the tower.

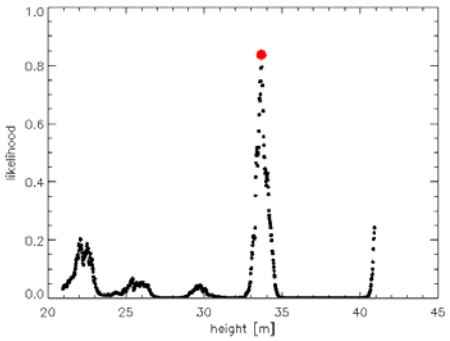

Figure 8: Likelihood of height in case of multiple scatterers in a resolution cell.

4 Summary

A new method for estimating the 3D scatterer location and resolution cell configuration has been developed. It is based on the principle of radargrammetry and uses Bayesian inference. It complements coherent techniques PSI and TomoSAR and is insensitive to temporal decorrelation, APS and non-linear motion of point scatterers.

For implementing this method, a new estimation framework has been developed. Firstly, directed graphs are used to represent dependencies of RVs. And secondly, pdfs are modelled by particle representations. The principle of radargrammetry is converted to a simple Bayesian line fitting problem. Demonstration using TerraSAR-X data for Berlin central station shows that this technique is capable of unambiguous height estimation of point scatterers and consequently, more precise surface displacement of urban areas is possible by combining this technique with PSI and TomoSAR.

The technique can take benefit from adding more incidence angles e.g. out of full performance range, converting amplitude images to likelihood images, future SAR systems with 600 MHz chirp bandwidth and prior information about height.

References

[1] Ferretti, A.; Prati, C.; Rocca, F.: *Permanent scatterers in SAR interferometry.* IEEE TGARS, Vol. 39, No. 1, pp. 8-20, 2001.

[2] Adam, N.; Bamler, R.; Eineder, M.; Kampes, B.: *Parametric estimation and model selection based on amplitude-only data in PS-interferometry.* Proc. of FRINGE'05, Frascati, on CD, 2005.

[3] Fornaro, G..; Monti Guarnieri, C.; Pauciullo, A.; Tebaldini, S.: *Joint multi-baseline SAR interferometry.* EURASIP J. Appl. Signal Process, vol. 20, pp. 3194–3205, 2005.

[4] Reigber, A.; Moreira, A.: *First demonstration of airborne SAR tomography using multibaseline L-band data.* TGARS, vol. 38, no. 5, pp. 2142-2152, 2000.

[5] Zhu, X.; Adam, N.; Bamler, R.: *Space-borne high resolution SAR tomography: Experiments in urban environment Using TS-X Data.* Proc. of Joint Urban 2009, Shanghai, 2009.

[6] Bamler, R.: *Interferometric stereo radargrammetry: Absolute height determination from ERS-ENVISAT interferograms.* Proc. of IGARSS, Hawaii, on CD, 2000.

[7] Bamler, R., Eineder, M.: *Accuracy of differential shift estimation by correlation and split bandwidth interferometry for Wideband and Delta-k SAR systems.* GRSL, vol. 2, pp.151-155, 2005.